

Identification of dark axisymmetric plasma modes in partially gated two-dimensional electron gas disk

M.V. Cheremisin

A.F.Ioffe Physical-Technical Institute, St.Petersburg, Russia

(Dated: June 14, 2023)

We investigate the dark axisymmetric plasmon spectrum for partially gated two-dimensional gas of the disk shape. The extension of the central gate spot leads to change in plasmon spectrum from square-root in wave vector to linear dispersion associated to the gated part along. Intriguingly, the interchange between neighboring modes occurs because of stepwise change in carrier screening across the circumference of the gate. This behavior is unexpected when changing from a fully screened to unscreened two-dimensional gas by increasing of the sub-gate gap [A.L.Fetter, Phys.Rev.B 33, 5221 (1986)]. Our results provide the accurate identification of axisymmetric plasmon modes recently observed in experiment and, in addition, pave the way for feedback plasmon resonator study.

Plasma oscillations in two-dimensional(2D) electron gas were first predicted in the 70th by F.Stern¹ for ungated and, then analyzed for gated systems². Over the next decade the plasmon assisted infrared absorption³⁻⁶ and emission⁷ has been reported. Since Stern's pioneering discovery the enormous efforts were done to clarify the plasmon behavior found to be influenced by magnetic field⁸⁻¹⁰, retardation effects¹¹, sample geometry¹²⁻¹⁴ and quality^{15,16}.

A decade ago it was shown¹⁷⁻¹⁹ that the plasma oscillations in two-dimensional systems with arbitrary attached gates and contacts can be elegantly described in terms of classical theory of electrical circuits with distributed parameters. The proposed LC-approach is extremely powerful for description of plasmon excitations in narrow stripes of 2D gas with periodic grating²⁰. Highly motivated by recent experiments dealt with axisymmetric plasmon excitations observed²¹⁻²³ in partially gated 2D disk we attempt to study this subject.

Let us consider two-dimensional electron system of disk geometry depicted by shaded area in Fig.1, inset. The 2D gas mesa of radius R is grounded peripherally and, moreover, embedded into an homogeneous dielectric environment with constant ϵ . The cylindrical slab of the height h is covered atop by gate of radius $r_0 \leq R$. For clarity, we further fix 2D mesa radius R and, then vary the sizes h, r_0 . We will be interested in study of axisymmetric plasmon modes known^{12,24,25} to have zero angular momentum $l = 0$. Conventionally, these modes are called "dark" because of weak coupling with external electromagnetic fields, hence difficulties in excitation(detection). Arguing that axisymmetric modes are purely radial we make use of LC-approach¹⁹ in order to find the plasmon spectra and, then compare theory predictions with experimental data^{21,22}.

In what follows we will use the quasistatic approximation¹², consisting of continuity and hydrodynamic Euler's equations. Aiming to analyze the existing experimental data^{21,22} we further demonstrate a negligible role of retardation effects. Instead of complete Maxwell's equation formalism²⁵, one may use non-retarded Poisson equation for searching the in-plan electric potential of 2D gas embedded into uniform dielectric environment. Following Ref.¹² the set of equations constituent the hydrodynamic model could be linearized with respect to small amplitude of plasma wave excitations. Fortunately, the model is greatly

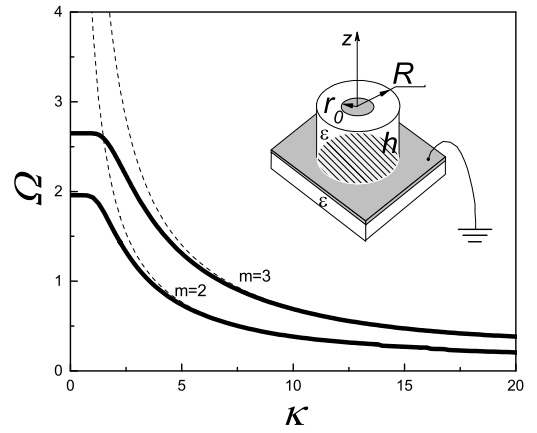


FIG. 1: Inset: the experimental setup. Main panel: the dimensionless frequency $\Omega = \omega/\omega_0$ vs screening parameter $\kappa = \sqrt{R}/2h$ for lowest plasma modes with $\alpha_{02} = 3.831$ and $\alpha_{03} = 7.016$ respectively for totally covered atop 2DEG, i.e. when $r_0 = R$. Dashed curves represent the asymptotes $\Omega = \frac{\alpha_{0m}}{\kappa}$ for highly screened 2D gas.

simplified leading to so-called telegraphist equations for radial components of in-plane potential U and the current I :

$$\frac{\partial U}{\partial r} = -L \frac{\partial I}{\partial t}, \quad (1)$$

$$\frac{\partial I}{\partial r} = -C \frac{\partial U}{\partial t}, \quad (2)$$

$$L(r) = \frac{m^*}{e^2 n} \frac{1}{2\pi r}, \quad C(r) = \frac{(1 + \coth(qh))\epsilon q r}{2}. \quad (3)$$

Here, L, C are the inductance and capacitance per unit length respectively, m^* and n are the effective mass and density of 2D carriers. Then, q is the plasmon wave vector originating from solution of the Poisson equation accounting the actual electrostatic environment.

We now search the solution of Eq.(1,2) separating the temporal and spatial components for potential $U = U(r) \exp(i\omega t)$ and current $I = I(r) \exp(i\omega t)$. Finally, the

equation for radial part of the potential yields:

$$\frac{d^2U}{d\rho^2} + \frac{1}{\rho} \frac{dU}{d\rho} + U = 0. \quad (4)$$

Here, we introduced the dimensionless radius $\rho = r/\lambda$, where $\lambda = \frac{1}{\omega\sqrt{LC}}$ is the length scale of the problem. The general solution of Eq.(4) is given by the sum of zero order Bessel functions of first(second) kind, namely

$$U(\rho) = AJ_0(\rho) + BY_0(\rho). \quad (5)$$

The arbitrary constants in Eq.(5) can be found by use of correct boundary conditions.

Let us first consider the simple case of totally gated 2D gas, i.e when $r_0 = R$ and variable height $0 < h < \infty$ of the slab. Arguing the potential is finite in the disk center we put $B = 0$ to avoid divergent behavior of the second term in Eq.(5) at $\rho \rightarrow 0$. Noticing that the peripheral current is absent, i.e. $I(R) \sim \rho \frac{dU}{d\rho} = 0$, we finally find out the dispersion equation for plasmon excitations

$$\omega\sqrt{LC}R = \alpha_{0m}. \quad (6)$$

Similar to Ref.¹² we will use the notation α_{0m} for m th zero of the function $J_0(x)$. Using Eq.(3) we re-write Eq.(6) as it follows

$$\omega = v_p \frac{\alpha_{0m}}{R} \cdot \left[\frac{1 - e^{-2hq}}{2hq} \right]^{1/2}, \quad (7)$$

where $v_p = \sqrt{\frac{4\pi e^2 nh}{m^* \epsilon}}$ is plasma wave velocity.

For strong screening case $qh \ll 1$ we obtain the relationship

$$\omega = v_p \frac{\alpha_{0m}}{R}, \quad (8)$$

which is exactly the linear dispersion law^{2,12} if one defines wave vector

$$q = \frac{\alpha_{0m}}{R} \quad (9)$$

for present case of axisymmetric plasmon excitations.

In the opposite ungated case $qh \gg 1$ Eq.(7) provides familiar long-wavelength dispersion law¹

$$\omega = \sqrt{\frac{2\pi e^2 n}{m^* \epsilon}} q \quad (10)$$

with the wave vector specified by Eq.(9) as well.

Let's do visualization of the transition from ungated to screened 2D system by fixing the disk radius and, then varying the slab height. It is convenient to introduce the reference value of frequency $\omega_0 = \sqrt{\frac{2\pi e^2 n}{m^* \epsilon R}}$ and screening parameter $\kappa = \sqrt{R/2h}$. Using Eq.(7) we plot in Fig.1 the dimensionless frequency $\Omega = \omega/\omega_0$ vs κ for lowest axisymmetric modes $m = 2, 3$. For highly screening case $\kappa \gg 1$ one obtains $\Omega = \frac{\alpha_{0m}}{\kappa}$ being a simple replica of Eq.(8). For ungated

2D gas $\kappa \ll 1$ we recover the result specified by Eq.(10) as $\Omega = \sqrt{\alpha_{0m}}$. The change in axisymmetric mode behavior occurs at $\kappa \sim 1$ which was not clearly indicated in longstanding classical study¹².

The second part of the present paper concerns more interesting case of partially gated 2D electron system shown in Fig.1, inset. The extension of the central gate spot would result in a transition from ungated to fully gated 2D gas as well. We now search the spectra of axisymmetric excitations by varying the central gate radius $0 \leq r_0 \leq R$ and keeping fixed h, R . Evidence shows that for gated disk(index "1") and ungated hoop(index "2") the in-plane potential can be written by Eq.(4) taking into account the respective capacitances specified by Eq.(3).

$$U_1 = A_1 J_0(\rho_1) \quad (11)$$

$$U_2 = A_2 J_0(\rho_2) + B_2 Y_0(\rho_2) \quad (12)$$

$$U_1 = U_2 |_{r=r_0}, U'_1 = U'_2 |_{r=r_0}, U'_2 |_{r=R} = 0, \quad (13)$$

where the dimensionless variable $\rho_{1,2} = r/\lambda_{1,2}$ are different for gated disk and ungated hoop since $\lambda_{1,2} = \frac{1}{\omega\sqrt{LC_{1,2}}}$.

Equations(11),(12) have to be solved jointly with boundary conditions specified by Eq.(13) for continuous potential and current in gated/ungated parts respectively and, then the absence of outgoing current at the slab perimeter. Finally, we obtain cumbersome transcendental dispersion equation

$$J_0(\Omega\kappa\nu)(J_1(\Omega^2\nu)Y_1(\Omega^2) - J_1(\Omega^2)Y_1(\Omega^2\nu)) + \frac{k}{\Omega} J_1(\Omega\kappa\nu) [J_1(\Omega^2)Y_0(\Omega^2\nu) - J_0(\Omega^2\nu)Y_1(\Omega^2)] = 0, \quad (14)$$

which can be minimized as it follows

$$D_U \cdot H_I + \frac{k}{\Omega} D_I \cdot H_U = 0. \quad (15)$$

Eq.(15) allows one to obtain the plasmon frequency Ω vs dimensionless radii ratio $\nu = r_0/R$ at certain value of screening parameter κ . Here, we use the notations $D_I = J_1(\Omega\kappa\nu)$ and $D_U = J_0(\Omega\kappa\nu)$ for gated disk(D) part. The solutions $D_{I(U)} = 0$ correspond to zero current at the disk center and, then the zero current(voltage) respectively at the disk circumference. The remaining multipliers, namely $H_I = J_1(\Omega^2\nu)Y_1(\Omega^2) - J_1(\Omega^2)Y_1(\Omega^2\nu)$ and $H_U = J_1(\Omega^2)Y_0(\Omega^2\nu) - J_0(\Omega^2\nu)Y_1(\Omega^2)$ correspond to ungated hoop(H) part seen in Fig.1, inset. The transcendental equations $H_{I(U)} = 0$ define the solution of Bessel Eq.(4) for zero current(voltage) respectively at the internal boarder and, then the absence of the current at the outer circumference of the hoop.

For real systems²² the typical disk size $R = 0.25\text{mm}$ is much grater that the gate to 2DEG separation is $h = 370\text{nm}$, hence we find $\kappa = 18 \gg 1$. Assuming that $\Omega \sim 1$ we conclude that second summand in Eq.(15) prevails. In general, the zeroth of transcendental equation $D_I = 0$ defines in total the solution of Eq.(15). The later condition corresponds to axisymmetric plasmon localized in a gated part along. It is easy to check that the plasmon frequencies are given by asymptotes

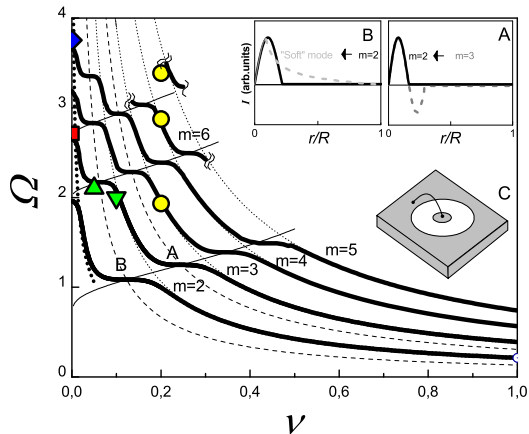


FIG. 2: The dimensionless frequency $\Omega = \omega/\omega_0$ vs ratio $\nu = r_0/R$ for lowest $m = 2..5$ and, partially $m = 6, 8$ plasma modes plotted for fixed $\kappa = 18$. Dotted lines represent the asymptotes $\Omega = \frac{\alpha_0 m}{\kappa \nu}$ expected for plasmon in the gated part along. Dashed(thin) lines depict $D_U = 0$ and $H_U = 0$ solutions respectively. Bold dashed line specifies the "soft" mode asymptote $\Omega = \frac{1}{\sqrt{\kappa \nu}}$. The experimental data for ungated ($\square^{22}, \diamond^{23}$) and partially gated ($\triangle, \nabla, \circ^{21}$) 2D systems is denoted in Table 1. Inset A(B): Radial distribution of the current density for and intermode transition A and B respectively shown in the main panel. Inset C: Feedback 2D plasmon resonator(under Ref.²⁶).

$\Omega = \frac{\alpha_0 m}{\kappa \nu}$ shown by dotted lines in Fig.2. However, this simple scenario fails when the multipliers from first(second) summand in Eq.(15) vanish simultaneously $D_U, H_U = 0$, therefore the dispersion Eq.(15) becomes fulfilled as well. The solutions of equations $D_U = 0$ and $H_U = 0$ are shown in Fig.2 by thin and dashed lines respectively. This condition $D_U, H_U = 0$ is exactly one defines the transition between neighboring axisymmetric modes. To support our reasoning we plot schematically in Fig.2, inset A the spatial distribution of the current for initial $m = 3$ and, then final $m = 2$ neighboring plasma modes. Actually, the transition $3 \rightarrow 2$ depicted as A in Fig.2 can be viewed as a plasma wave that loses half of the period.

For small gate sizes when the most place atop the slab is occupied by ungated hoop, the lowest mode $m = 2$ undergo further transformation. The point of interest B in Fig.2 is still defined by condition $D_U, H_U = 0$. However, in the present case the plasmon mode $m = 2$ is first confined within ultra-narrow gated part and, then is modified entirely by occupation of the ungated part as whole. Let us call further this mode as "soft" mode. In Fig.2 we represent schematically the current spatial distribution for initial $m = 2$ mode and, finally, the "soft" mode. We verify the dispersion relation for "soft" mode follows the asymptote $\Omega = \frac{1}{\sqrt{\kappa \nu}}$. In actual fact, the appearance of the "soft" mode is a precursor of the conventional plasmon in totally ungated 2D disk, i.e. when $\Omega = \sqrt{\alpha_0 m}$.

It is worthwhile to mention with respect to Fig.2 that upon change of the gated part radius r_0 the plasmon frequency fol-

lows either $\omega \sim 1/\sqrt{r_0}$ or $\omega \sim 1/\sqrt{R}$ dependencies regarding to the actual ν -range of interest. Evidently, this uncertainty may lead in misunderstanding regarding accurate identification of the plasmon modes. We argue that the present model would be useful for analyzing the axisymmetric plasmon excitations persisting in partially gated 2D disk feedback system²⁶ shown in Fig.2,inset.

TABLE I: Axisymmetric plasmon: theory vs experiment

Samp.	$n \cdot 10^{11}$ [cm ⁻²]	h [nm]	r_0 [mm]	R [mm]	f_0 [GHz]	A	f_{exp} [GHz]	Ω_{exp}	Ref.
N1	2.6	-	0	0.25	22.1	0.41	60.0	2.7	\square^{22}
N2	1.0	370	0.05	1.0	6.9	0.51	14.4	2.1	\triangle^{21}
N3	1.0	370	0.05	0.50	9.7	0.36	19.4	2.0	∇^{21}
N4	1.0	370	0.05	0.25	13.7	0.26	26.5	1.9	\circ^{21}
N4	1.0	370	0.05	0.25	13.7	0.26	39.4	2.9	\circ^{21}
N4	1.0	370	0.05	0.25	13.7	0.26	46.4	3.5	\circ^{21}
N5	1.0	-	0	0.50	9.7	0.36	36.4	3.7	\diamond^{23}

Let us compare our results with experimental data for Al-GaAs/GaAs samples($\epsilon = 12.8$) demonstrated²¹⁻²³ axisymmetric plasmon excitations. At first, we calculate the reference frequency $f_0 = \omega_0/2\pi$ for each specimen presented in Table 1. To confirm validity of our quasistatic approach, we calculate the ratio of the long-wavelength plasma frequency to light frequency with the same wave vector, $A = \omega_0 \sqrt{\epsilon} R/c$, called retardation parameter¹¹. For all samples in Table 1 $A \ll 1$. We conclude that retardation effects are insignificant therefore use of non-retarded Poisson's equation is well justified.

Continuing the analysis of experimental data we calculate the dimensionless ratio $\Omega_{\text{exp}} = f_{\text{exp}}/f_0$ for each sample. The resulting data points are then added to the graph of plasmon spectra in Fig.2. Remarkably, the experimental values match perfectly the certain modes of axisymmetric plasmon spectrum. For samples N1,2,3 the lowest observed plasmon mode corresponds to $m = 3$. Then, the sample N4 demonstrated a series of even-numbered plasmon modes $m = 4, 6, 8$. The ungated sample N5 exhibited the plasma mode for $m = 5$. In all cases, expected strong the fundamental axisymmetric mode $m = 2$ was not observed. Although this finding looks puzzling, the answer is unpretentious. Recall that for dark axisymmetric plasmon excitation the coupling with external electromagnetic radiation is much weaker²¹ compared to conventional plasmons with nonzero angular momentum $l \neq 0$. Hence, the dark modes would be hidden out by conventional ones. Indeed, the conventional $l = 1$ modes observed²² at frequencies 18GHz and 13GHz cover the spectral range of axisymmetric fundamental modes expected at 13.6GHz and 10.4GHz for samples N4 and N3 respectively. For ungated sample N1 the calculation for dark mode $m = 2$ gives frequency 43GHz which close to 39GHz reported²¹ for conventional plasmon mode $l = 2$. Finally, for sample N5 one expect the fundamental dark mode at 18.8 GHz which coincides²³ with conventional mode $l = 1$ at 19GHz.

In conclusion, we investigated the transition from ungated

to gated two-dimensional system of disk geometry by means of central spot gate expansion. The discontinuity of gated to ungated part provides the interchange between the neighboring axisymmetric modes. The experimental data for different

sample sizes, carrier densities is found to agree well with theory predictions. Our study allows to classify the observed dark axisymmetric modes and, moreover, pave a way to feedback plasmon resonator²⁶ study.

-
- ¹ F. Stern, Phys. Rev. Lett. **18**, 546 (1967).
² A.V. Chaplik, Zh. Eksp. Teor. Fiz. **62**, 746 (1972) [Sov. Phys. JETP **35**, 395 (1972)].
³ C.C. Grimes and G. Adams, Phys. Rev. Lett. **36**, 145 (1976).
⁴ S.J. Allen, D.C. Tsui and R.A. Logan, Phys. Rev. Lett. **38**, 98 (1977).
⁵ T.N. Theis, J.P. Kotthaus and P.J. Stiles, Solid State Commun. **26**, 603 (1978).
⁶ D.Heitmann, J.P. Kotthaus, and E.G. Mohr, Solid State Commun. **44**, 715 (1982).
⁷ D.C. Tsui, E. Gornik, and R.A. Logan, Solid State Commun. **35**, 875 (1980).
⁸ K.W. Chiu and J.J.Quinn, Phys. Rev. B **9**, 4724 (1974).
⁹ M. Nakayama, J.Phys. Soc. Jpn. **36**, 393 (1974).
¹⁰ V.A. Volkov and S.A. Mikhailov, Sov. Phys. JETP **67**, 1639 (1988).
¹¹ I.V. Kukushkin, J.H. Smet, S.A. Mikhailov, D.V. Kulakovskii, K.von Klitzing and W. Wegscheider, Phys. Rev. Lett. **90**, 156801 (2003).
¹² A.L. Fetter, Phys. Rev. B **33**, 5221 (1986).
¹³ Yu.A. Kosevich, A.M. Kosevich, J.C. Granada, Phys. Lett. A, **127**, 52 (1988).
¹⁴ A.A. Zabolotnykh and V.A. Volkov, Pis'ma Zh. Eksp. Teor. Fiz. **115**, 163 (2022) [JETP Lett. **115**, 141 (2022)].
¹⁵ V.I. Falko and D.E.Khmel'nitskii, Zh. Eksp. Teor. Fiz. **95**, 1988 (1989) [Sov. Phys. JETP **68**, 1150 (1989)].
¹⁶ M.V. Cheremisin, Solid State Commun. **268**, 7 (2017).
¹⁷ P.J. Burke, I.B. Spielman, and J.P. Eisenstein, Appl. Phys. Lett. **76**, 745 (2000).
¹⁸ F. Rana, IEEE Trans. Nanotech. **7**, 91 (2008).
¹⁹ G.C. Dyer, G.R. Aizin, S. Preu, N.Q. Vinh, S.J. Allen, J.L. Reno, and E.A. Shaner, Phys. Rev. Lett. **109**, 126803 (2012).
²⁰ G.C. Dyer, G.R. Aizin, S.J. Allen, A.D. Grine, D. Bethke, J. L. Reno, and E.A. Shaner, Nature Photon. **7**, 925 (2013).
²¹ V.M. Muravev, I.V. Andreev, V.N. Belyanin, S.I. Gubarev, and I.V. Kukushkin, Phys. Rev. B **96**, 045421 (2017).
²² A.A. Zagitova, V.M. Muravev, P.A. Gusikhin, A.A. Fortunatov, I.V. Kukushkin, Pis'ma Zh. Eksp. Teor. Fiz. **108**, 478 (2018) [JETP Lett. **108**, 446 (2018)].
²³ A.M. Zarezin, D. Mylnikov, A.S. Petrov, D. Svintsov, P.A. Gusikhin, I.V. Kukushkin, V.M. Muravev, Phys. Rev. B **107**, 075414 (2023).
²⁴ I.V. Zagorodnev, D.A. Rodionov and A.A. Zabolotnykh, Phys. Rev. B **103**, 195431 (2021).
²⁵ D.A. Rodionov, I.V. Zagorodnev, A.A. Zabolotnykh, and V.A. Volkov, J. Phys.: Conf. Ser. **1686**, 012052 (2020).
²⁶ V.M. Muravev, P.A. Gusikhin, A.M. Zarezin, A.A. Zabolotnykh, V.A. Volkov and I. V. Kukushkin Phys. Rev. B **102**, 081301(R) (2020).